Germanium Nanostructures on Silicon Observed by Scanning Probe Microscopy

Masahiko Tomitori and Toyoko Arai

Abstract

Scanning tunneling microscopy and noncontact atomic force microscopy have been used to observe germanium growth on Si(001) and Si(111). The atomically resolved images provide invaluable information on heteroepitaxial film growth from the viewpoints of both industrial application and basic science. We briefly review the history of characterizing heteroepitaxial elemental semiconductor systems by means of scanning probe microscopy (SPM), where the Stranski–Krastanov growth mode can be observed on the atomic scale: the detailed phase transition from layer-by-layer growth to three-dimensional cluster growth was elucidated by the use of SPM. In addition, we comment on the potential of SPM for examining the spectroscopic aspects of heteroepitaxial film growth, through the use of SPM tips with well-defined facets.

Keywords: *AFM, atomic force microscopy, crystal growth, elemental semiconductors, germanium, nanostructures, scanning probe microscopy, scanning tunneling microscopy, silicon, SPM, STM.*

Introduction

It is widely accepted that scanning probe microscopy (SPM)[1] has greatly contributed to the development of nanoscale materials science and technology. Using SPM, we can obtain information on surface topography and simultaneously measure the physical properties of the surface with atomic resolution. In the early 1980s, the advent of scanning tunneling microscopy (STM)[2] as the first member of the SPM family of techniques was a landmark achievement in the field of high-resolution microscopies: a mechanically sharpened tip was able to precisely depict a sample surface with atomic resolution. Moreover, the more recent technique of noncontact atomic force microscopy (nc-AFM)[3,4] can also achieve atomic resolution, even on low-conductivity and insulating materials;[5] this noticeable feature has not been achieved by any other microscopic technique to date. With SPM, the development of a mechanical scanning method using an atomically sharp tip is leading us into a fascinating "nanoworld."

In materials science and technology on the nanoscale, the fabrication and evaluation of heteroepitaxial nanostructures have attracted much interest for realizing novel optoelectronic devices, in particular, by direct observation and manipulation using SPM. In general, nanostructures fabricated on surfaces are surrounded by characteristic crystallographic small planes (i.e., facets) in such a way that the total energy around the nanostructures decreases under pseudo-equilibrium conditions. In principle, the optoelectronic properties concerning quantum states—for example, light emission with a blueshift—are governed by the shape, atomic arrangement, and composition of nanostructures. Thus, three-dimensional (3D) topographic observation is indispensable for characterizing the properties of faceted nanostructures and designing and creating novel functional devices using them. It is not easy to observe nanostructures with complicated facets, but SPM makes it possible, as does low-energy electron microscopy (LEEM).[6] Although LEEM has advantages in analyzing nanostructure facets in real time without any tip-induced artifacts,[7] SPM is superior to LEEM in regard to the achievable spatial resolution, and the two techniques can be used complementarily.

A typical example for heteroepitaxial crystal growth leading to the self-organized formation of nanostructures is to be found in the Si-Ge system. Extending the capabilities of Si as the most widely used semiconducting material is of great importance from an industrial viewpoint. The integration of other materials can provide a Si-containing material with light-emitting and fast-switching capabilities. Integration has been carried out by fabricating hetero-interfaces, quantum dots, and superlattices on Si. Germanium deposited on a Si(001) surface exhibits pronounced features in growth mode: it was previously known from electron microscopy and electron diffraction studies that a Ge film deposited on Si(001) grows layer-by-layer up to a critical thickness of about three monolayers, and that sequentially, large Ge clusters form three-dimensionally beyond that critical thickness. This heteroepitaxial growth is categorized as the so-called Stranski–Krastanov growth mode, according to a simple classification usually employed in the field of heteroepitaxial crystal growth.[8] Since there is a lattice mismatch of 4.2% between Si and Ge, the interface between the Si and Ge surfaces is significantly strained. The strain energy is released by forming Ge clusters on the wetted layers with a critical Ge thickness to prevent the strain energy in the layers from piling up: the relaxation of the Ge atomic configuration in the growing cluster and on the surface of the cluster with various steps can decrease the total strain energy through gradual, slight deformation. This morphological change in the heteroepitaxial growth has not only invoked practical issues in the control of the Si-Ge interface, but also has initiated a debate in the materials science community concerning heteroepitaxial cluster growth in preferential shapes with respect to energetics. SPM provides extremely valuable images for analyzing this type of heteroepitaxial growth with atomic resolution.[9]

Furthermore, a well-defined nanostructure with specified facets and atomic reconstruction is required for establishing a standard tip for SPM. For atomic-resolution

imaging by STM, an atomically sharp tip with a stable structure is required. However, to measure the physical properties of a sample (i.e., the surface electronic states and the force interaction between the tip and the sample), the atomic species at the apex of the tip and the structure of the shank should be well defined; we always measure the quantity convolutedly related to the electronic properties of both the tip and the sample. A well-defined tip having an apex surrounded with specified facets can promote theoretical studies of the interaction between the tip and the sample. In this review, we mainly describe Ge cluster growth on Si substrates in various modes observed by SPM, and discuss the advantages of SPM tips with well-defined facets from the viewpoint of nanoscale materials science.

STM Observation of the Stranski–Krastanov Growth Mode: Ge Clusters on Si

In the 1980s, Si(111) and Si(001) surfaces played an important role in confirming and demonstrating the atomic resolution of the STM instruments developed in laboratories around the world.[10] Afterward, many researchers started to observe molecular adsorption and thin-film growth on these surfaces, as well as Si growth on Si. Subsequently, in the early 1990s many researchers started to observe the heteroepitaxial thin-film growth of semiconductors by STM, in particular, Ge on a Si(001) substrate.[11–18] Ge crystals have the same diamond structure as Si, in which each atom has four bonds with one electron per bond. Thus, in principle, initial growth of less than one monolayer (ML) of Ge on Si exhibits a similar topography to Si overlayers on Si.

Figure 1a shows a simplified model of a Si(001) 2×1 reconstructed surface consisting of symmetrical Si dimers with monoatomic height steps: this surface has a periodicity of two times the primitive cell on an ideal Si(001) diamond surface. One dimer consists of two Si atoms bound to each other; by forming a dimer, the number of dangling bonds at each Si atom on the surface is reduced by one-half, while increasing the strain energy through tilted bonds, resulting in a stable arrangement with the lowest surface energy. To be precise, the dimer achieves this lower energy by asymmetrically buckling, with one Si atom up and the other Si atom down. The two atoms in an asymmetrical dimer can quickly flip-flop between buckling up and down at room temperature, and consequently, the dimer looks symmetrical on a time-averaged basis using STM, which has a slow response time[19] (Figure 1b). The Si dimers form a row, leading to a 2×1 reconstruction with respect to the primitive surface cell of the (001) plane. On the upper terrace, the dimer rows run perpendicular to those on the lower terrace. This arrangement conforms in a reasonable manner to the dimer formation on a stepped surface of a diamond structure: the dimer orientation is rotated 90° on the upper terrace with respect to the lower terrace, with a monoatomic step height.

Figure 2 shows an STM image of a Ge-deposited Si(001) surface at 300°C with a Ge coverage of <0.1 ML. The Ge dimers are depicted as bright protrusions, and some of them form a line: a buckled-up Ge atom in a dimer clearly protrudes in the image, and some isolated Ge dimers look symmetrical with a depression at the middle of the dimer, corresponding to a node of electronic states.[13,16] The Ge dimers in the line exhibit asymmetry as a zigzag pattern, and the asymmetry is also induced in the surface regions of Si without Ge coverage. This means that the Ge deposition freezes the flip-flop motion of Si dimers on the substrate by means of the induced strain. By increasing Ge deposition up to 1 ML, the surface becomes covered with Ge dimers, while the Ge dimers form rows that meet each other at many places over the substrate. Beyond 1 ML Ge coverage, missing-dimer rows are introduced to decrease the surface strain, as has been explained by Köhler et al.;[15] generally speaking, a Ge atom, with a radius larger than that of Si, cannot enter the narrow missing-dimer rows. Figures 3a and 3b show STM images of 2 ML and 3.5 ML Ge coverage, respectively, grown at 500°C. The missing-dimer rows appear as dark lines in Figure 3a and are regularly introduced in Ge layers with a periodicity of 8–10 dimers in a belt-like structure.[17] In Figure 3b, the patch-like structures found at about 3.5 ML Ge coverage are combinations of perpendicularly crossing missing-dimer rows. The Ge atoms deposited on the belt-like structure cannot be adsorbed in the missing-dimer row due to an increase in strain energy. This leads to the formation of a Ge dimer colony in a "patch" area, surrounded by missing-dimer rows: missing-dimer rows in the layer underneath look like trenches, and the dark rows running perpendicular to them are newly formed missing-dimer rows generated by the Ge overgrowth.

Further Ge deposition initiates 3D Ge cluster growth. Figure 4 shows an STM image of 3 ML Ge coverage at 300°C, exhibiting precursor nuclei for Ge cluster growth over a few patches. Proceeding with Ge deposition, we observe the formation of many "hut" clusters, first found by Mo et al.,[11] as shown in Figure 5a. Each hut cluster has four {015} facets with ridge lines at the meeting of two facets and a narrow (001) top consisting of dimer rows. The {015} facet has perfectly regular atomic rows. Tomitori et al. found that Ge growth on Si(015) continues layer-by-layer beyond

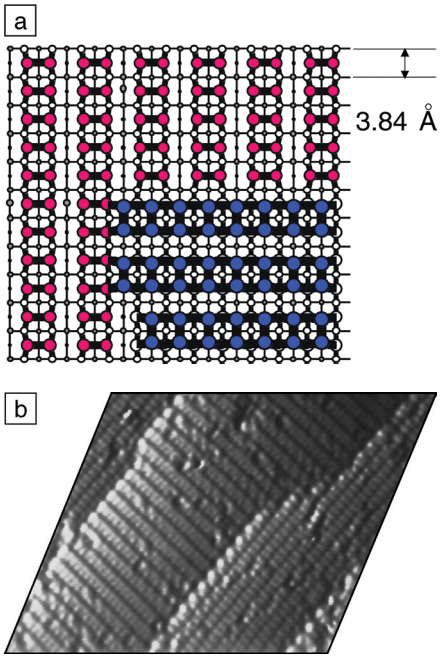

Figure 1. (a) Simplified atomistic model of a Si(001) 2×1 surface consisting of symmetrical Si dimers. Red circles correspond to atoms on the lower terrace, and blue circles correspond to atoms on the upper terrace, at a height difference of a monoatomic step (~0.14 nm). (b) Typical scanning tunneling microscopy image of a Si(001) 2×1 surface at a sample bias voltage of –1 V with respect to the tip potential. The scanning area is approximately 20 nm × 15 nm.

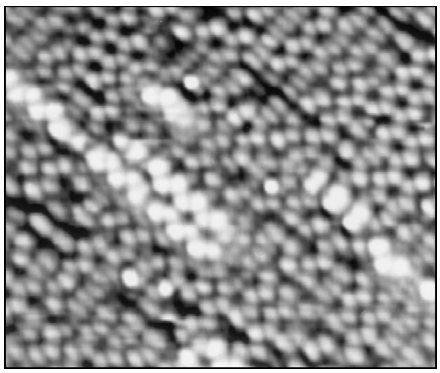

Figure 2. Scanning tunneling microscopy image of Ge dimers on a Si(001) surface at 300°C with a Ge coverage of <0.1 ML. The Ge dimers are depicted as bright protrusions; the scanning area is approximately 13 nm × 10 nm.

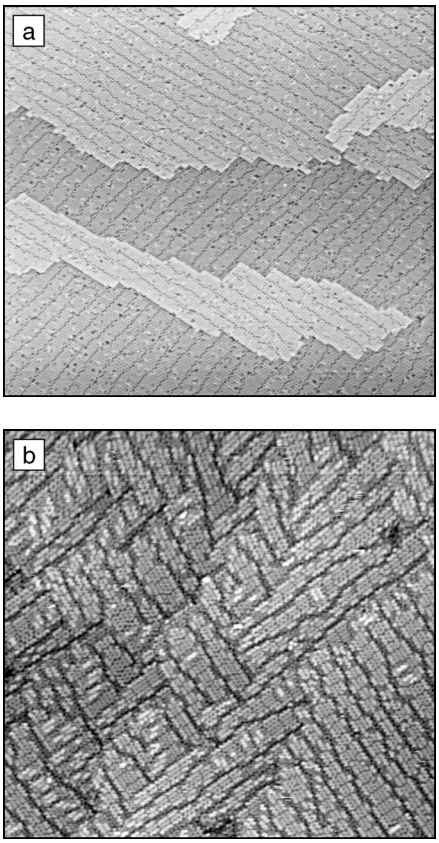

Figure 3. Scanning tunneling microscopy images of (a) ~2 ML Ge coverage with a belt-like structure (scanning area, approximately 100 nm × 90 nm), and (b) 3.5 ML Ge coverage with a patch-like structure (scanning area, approximately 70 nm × 70 nm), both grown at 500°C and observed at room temperature.

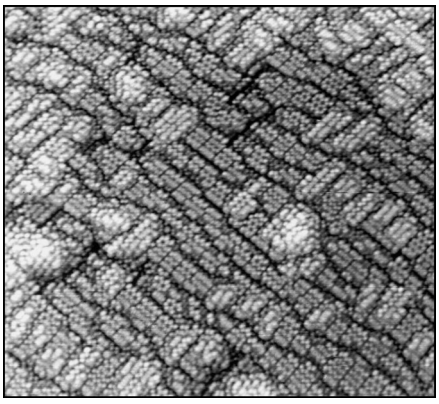

Figure 4. Scanning tunneling microscopy image of 3 ML Ge coverage at 300°C, exhibiting precursor nuclei for three-dimensional Ge cluster growth. Scanning area, approximately 45 nm × 45 nm.

10 ML with almost no defects.[20] This surface is regarded as a small (001) terrace repeating with a single-atom-height step and a 45°-rotated two-dimer width. Thus, the strain in the heteroepitaxial growth can be released through the step, which has a more flexible atomic configuration. A detailed atomic configuration model has recently been proposed by Fujikawa et al.[21] and confirmed using density functional theory calculations by Hashimoto et al.[22] The rebonding configuration is introduced at the step of the small (001) terrace to stabilize the electronic states: back bonds of Ge atoms at the step edge are bound to dangling bonds of Ge dimer atoms on the lower terrace. This configuration was also discussed by Tomitori to explain defect-free Ge growth on Si(015).[20]

As shown in Figure 5b, larger Ge clusters with fourfold symmetry were found using STM; they were termed "dome" clusters by Tomitori.[17] The dome is surrounded by a (001) facet on the top, and by {113}, {015}, and other high-index facets in fours, due to the symmetry.

The surface phase transitions for Ge coverage of less than 10 ML at growth

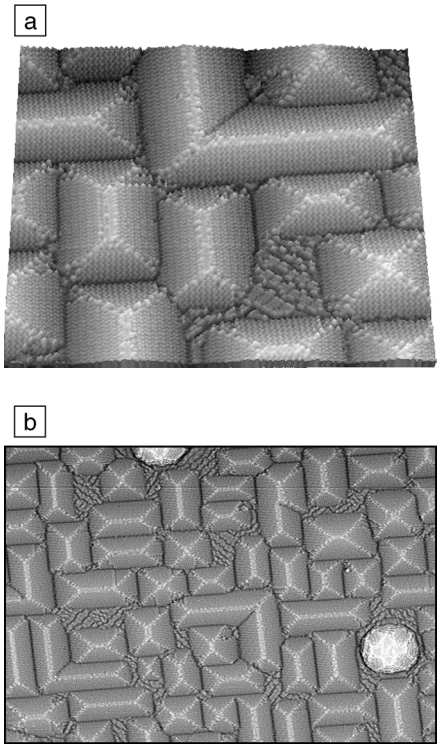

Figure 5. Scanning tunneling microscopy images of 6.5 ML Ge coverage grown at 500°C. (a) Ge "hut" clusters. Scanning area, approximately 70 nm × 70 nm. (b) Round "dome" clusters surrounded by hut clusters. Scanning area, approximately 200 nm × 150 nm.

temperatures of 300°C, 400°C, and 500°C are summarized in Reference 17. In that study, several large clusters were observed by annealing the sample. At the base of the clusters, close to the substrate, {015} facets always appear, probably to effectively reduce the strain energy at the interface between Si and Ge by introducing {015} facets with many (001) steps. Medeiros-Ribeiro et al.[23] statistically analyzed the abrupt volume change from "pyramid" clusters (hut clusters with a square base) to dome clusters, with few intermediate volume sizes, as a thermodynamic phase transition with an energy barrier, as evaluated from STM images of Ge on Si(001). On the other hand, Tromp et al. clearly observed the transition from pyramid to dome clusters in real time at high temperatures by LEEM and concluded that the shape change is due to an anomalous coarsening process similar to Ostwald ripening, with a slow transformation via several transition states.[24] Although Voigtländer succeeded in observing hut cluster growth at high temperatures by fast STM,[9] it is not easy to record the images at a video rate, particularly for rough surfaces [e.g., dome clusters on Si(001)]. Thus, complementary observations by LEEM and STM are a promising approach for studying heteroepitaxial growth proceeding by means of complicated modes such as the Stranski–Krastanov mode; LEEM is best for fast observations over wide areas, and STM for imaging with atomic spatial resolution.

Over the past few years, noncontact-AFM (nc-AFM) has become one of the most powerful atomic-resolution microscopies. Recently, the nc-AFM technique has been applied to studies of Ge on Si(111). Atomic-resolution images were obtained,[25] as shown in Figure 6. The reconstructions of 7×7, 5×5, and 9×9 unit cells, explained by the DAS model,[26] and their domain boundaries, as well as islands and step-flow growth, are observed as clearly as by STM (for example, see Reference 9). Using the interaction between the sample and a Si tip on an nc-AFM cantilever, we can observe the topography as well as simultaneously measure tunneling current and damping energy. The damping energy is a nanomechanical quantity that can be measured as the power input to a modulation piezo necessary to maintain a constant oscillation amplitude of the AFM cantilever. These simultaneously measured quantities provide us with surface spectroscopic information.

By changing the bias voltage between the tip and the sample, one can sometimes spontaneously modify the tip properties. When this occurs, the atomic contrast in nc-AFM topography and damping energy drastically changes: three Si corner adatoms

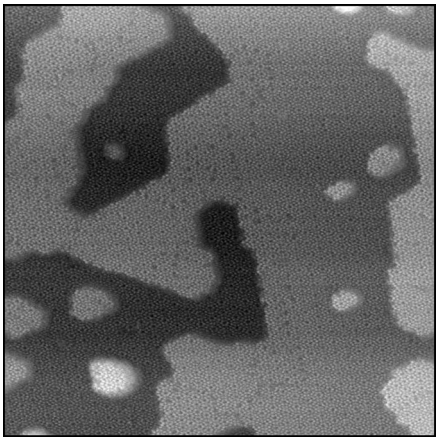

Figure 6. Noncontact atomic force microscopy image of Ge on Si(111) with Ge coverage of 0.7 ML grown at 450°C. Ge islands and step flow with 5 × 5, 7 × 7, and 9 × 9 unit cell reconstructions are observed. Darker areas correspond to the Si(111) 7 × 7 substrate without Ge coverage. The scanning area is approximately 75 nm × 75 nm.

on the faulted half of a 7 × 7 unit cell are distinctly depicted; moreover, in the damping image, one observes the three adatoms at specified sites in Ge overlayers.[25] This might indicate that nc-AFM can be used to distinguish Si and Ge at surfaces. It should also be noted that tip modification sometimes occurs accidentally when the tip is scanned over a sample.

To clarify the capabilities of nc-AFM, we should discuss the effect of bias voltage on the image contrast and the interaction change induced by the characteristics of the tip apex. We have suggested that a change in bias voltage shifts the Fermi levels in the tip and the sample and subsequently enhances a quantum mechanical resonance interaction between the energetically tuned surface states of the tip and the sample.[27] Furthermore, the background force changed by applying a bias voltage alters the imaging conditions, resulting in a contrast change and sometimes a contrast inversion.[28] The imaging mechanism of damping energy is still under debate in the field of nc-AFM.[4,29] Recently, Morita et al. distinguished Si and Ge atoms in a Si and Ge intermixing layer by nc-AFM: they reported that the difference in electronic states between Si and Ge atoms alters the interaction with a Si tip[30] under their conditions, compensating the difference in contact potential between the tip and the sample. On the other hand, Kawamura et al. reported a contrast change due to Si and Ge on the surface of step-flow superstructures covered with Bi observed by STM, which may be ascribed to the different electronic state of the Bi overlayer.[31] Intermixing Ge into a Si layer plays an important role in releasing the mismatch strain; recognition of Si and Ge atoms in the mixing layer by SPM is becoming increasingly important for heteroepitaxial systems.

The tip shape and composition are much more critical in forming atomic contrast in nc-AFM images than they are with STM: the chemical bonding states are governed by the electronic states of both the tip and the sample on the atomic scale. To elucidate the imaging mechanism for atomic contrast, the tip apex should be controlled in a well-defined manner. We usually use a commercially available [001]-oriented Si tip on a piezoresistive Si cantilever for nc-AFM. The tip can be heated in ultrahigh vacuum by passing a small current through the piezoresistive cantilever.[32,33] Nanoclusters with well-defined facets, such as the Ge hut and dome clusters on Si(001), are suitable candidates for an nc-AFM tip: Ge or a similar material deposited on a [001]-oriented Si tip and subsequently heated can lead to the formation of a well-defined tip surrounded by atomically flat facets having sharp corners at the meeting points of the facets. This process looks promising as an addition to traditional surface science methods for fabricating well-defined tips.

Summary

Scanning probe microscopy studies of a heteroepitaxial elemental semiconductor system [Ge on Si(001) and Si(111)] have been briefly described in this article, as well as the potential of SPM for studying heteroepitaxial film growth. The atomically resolved images obtained by SPM inspire us to understand nanostructures fabricated by heteroepitaxial growth; the complicated growth stages, referred to collectively as the Stranski–Krastanov growth mode, have been elucidated on an atomic scale by SPM. By finding initially grown facets on a wetting layer in the Stranski–Krastanov mode using SPM, we can choose a substrate having the same plane indexes as the facet to control overlayer morphology layer-by-layer—for example, the {015} facet of Ge on Si(001). In addition, an SPM tip with a reproducible and well-defined shape and composition can be fabricated by utilizing strained heteroepitaxial overlayers. These advances will open the way for the detailed analysis and fabrication of nanomaterials with new functional optoelectronic properties.

References

1. For example, see R. Wiesendanger, *Scanning Probe Microscopy and Spectroscopy: Methods and Applications* (Cambridge University Press, Cambridge, UK, 1994).
2. G. Binnig, H. Rohrer, Ch. Gerber, and E. Weibel, *Phys. Rev. Lett.* **49** (1982) p. 57.
3. F.J. Giessibl, *Science* **267** (1995) p. 68.
4. S. Morita, R. Wiesendanger, and E. Meyer, eds., *Noncontact Atomic Force Microscopy* (Springer-Verlag, Berlin, 2002).
5. M. Reichling and C. Barth, *Phys. Rev. Lett.* **83** (1999) p. 768.
6. E. Bauer, *Rep. Prog. Phys.* **57** (1994) p. 895.
7. For example, see M. Tomitori, F. Iwawaki, N. Hirano, F. Katsuki, and O. Nishikawa, *J. Vac. Sci. Technol., A* **8** (1990) p. 222.
8. For example, see C. Ratsch and A. Zangill, *Surf. Sci.* **293** (1993) p. 123.
9. B. Voigtländer, *Surf. Sci. Rep.* **43** (2001) p. 127.
10. R. Becker and R. Wolkow, in *Scanning Tunneling Microscopy,* Chapter 5, edited by J.A. Stroscio and W.J. Kaiser (Academic Press, San Diego, 1993) p. 149.
11. Y.-W. Mo, D.E. Savage, B.S. Swartzentruber, and M.G. Lagally, *Phys. Rev. Lett.* **65** (1990) p. 1020.
12. F. Iwawaki, M. Tomitori, and O. Nishikawa, *Surf. Sci. Lett.* **253** (1991) p. L411.
13. F. Iwawaki, M. Tomitori, and O. Nishikawa, *Surf. Sci.* **266** (1992) p. 285.
14. F. Iwawaki, M. Tomitori, and O. Nishikawa, *Ultramicroscopy* **42-44** (1992) p. 902.
15. U. Köhler, O. Jusko, B. Müller, M. Horn-von Hoegen, and M. Pook, *Ultramicroscopy* **42-44** (1992) p. 832.
16. M. Tomitori, K. Watanabe, M. Kobayashi, F. Iwawaki, and O. Nishikawa, *J. Vac. Sci. Technol., B* **12** (1994) p. 2022.
17. M. Tomitori, K. Watanabe, M. Kobayashi, and O. Nishikawa, *Appl. Surf. Sci.* **76/77** (1994) p. 322.
18. J. Knall and J.B. Pethica, *Surf. Sci.* **265** (1992) p. 156.
19. R.A. Wolkow, *Phys. Rev. Lett.* **68** (1992) p. 2636.
20. M. Tomitori, K. Watanabe, M. Kobayashi, and O. Nishikawa, *Surf. Sci.* **301** (1994) p. 214.
21. Y. Fujikawa, K. Akiyama, T. Nagao, T. Sakurai, M.G. Lagally, T. Hashimoto, Y. Morikawa, and K. Terakura, *Phy. Rev. Lett.* **88** 176101-1 (2002).
22. T. Hashimoto, Y. Morikawa, Y. Fujikawa, T. Sakurai, M.G. Lagally, and K. Terakura, *Surf. Sci.* **513** (2002) p. L445.
23. G. Medeiros-Ribeiro, A.M. Bratkovski, T.I. Kamins, D.A.A. Ohlberg, and R.S. Williams, *Science* **279** (1998) p. 353.
24. F.M. Ross, R.M. Tromp, and M.C. Reuter, *Science* **286** (1999) p. 1931.
25. T. Arai and M. Tomitori, *Appl. Surf. Sci.* **188** (2002) p. 292.
26. K. Takayanagi, Y. Tanishiro, M. Takahashi, and S. Takahashi, *J. Vac. Sci. Technol.,* **A3** (1985) p. 1502.
27. T. Arai and M. Tomitori, *Jpn. J. Appl. Phys., Part 1* **39** (2000) p. 3753.
28. T. Arai and M. Tomitori, *Appl. Surf. Sci.* **157** (2000) p. 207.
29. T. Arai and M. Tomitori, *Appl. Phys. A* **72** (2001) p. S51.
30. S. Morita and Y. Sugawara, in *Nanotechnology and Nano-Interface Controlled Electronic Devices*, Chapter 21, edited by M. Iwamoto, K. Kaneko and S. Mashiko (Elsevier, Amsterdam, 2002) p. 431.
31. M. Kawamura, N. Paul, V. Cherepanov, and B. Voigtländer, *Phys. Rev. Lett.* **91** 096102 (2003).
32. T. Arai and M. Tomitori, *Jpn. J. Appl. Phys., Part 1* **36** (1997) p. 3855.
33. T. Arai and M. Tomitori, *J. Vac. Sci. Technol., B* **18** (2000) p. 648. □